Electronic Supplementary Material (ESI) for Soft Matter.
This journal is © The Royal Society of Chemistry 2018

Supporting Information

Reversible Solvent-Sensitive Actuator with Continuous Bending/Debending Process from Liquid Crystal Elastomer-Colloidal

Yuanyuan Shang,[ab] Junchao Liu,[bc] Manbo Zhang,[a] Wanli He,[d] Xinyu Cao,[e] Jingxia Wang,*[bc] Tomiki Ikeda[b] and Lei Jiang[bc]*

1. Experimental Section

1.1 Materials

LC monomer A6OCB, LC cross-linker C6M and photo-initiator 2959 were purchased from Beijing Bayi Space LCD Technology Co. The raw materials for synthetic polyimide such as 4,4'-Biphthalic anhydride, 1-Methyl-2-pyrrolidinone, 4,4'-Oxydianiline and γ-Butyrolactone were purchased from J&K Scientific Ltd. Dichloromethane, chloroform, 1,2-dichloroethane and THF were purchased from the Beijing chemical plant.

1.2 Fabrication of colloidal template

It included the synthesis of monodisperse latex particles of P(St-MMA-AA), cleaning of glass and beaker and diluted latex particles solution. Firstly, the glass slides with dimension of 3.5 cm × 1.5 cm were rinsed and plasma treated to be superhydrophilic. Then the colloidal template was obtained by immersing the clean glass slide into the poly(St-MMA-AA) latex suspension with concentration of 0.5 wt% by vertical deposition at 60℃ with humidity of 60% RH for about 24 h.

1.3 Statement for the movie

Movie S1: Circle/multicircle actuation by dichloromethane. Film length: 6 mm, width: 1 mm, thickness: 15 μm, molar ratio of A6OCB/C6M: 10, at real time

Movie S2: Helix actuation by dichloromethane. Film length: 6 mm, width: 1 mm, thickness: 15 μm, molar ratio of A6OCB/C6M: 10, at real time

Movie S3: The deformation of the film when being removed from the solvent. Film length: 6 mm, width: 1 mm, thickness: 15 μm, molar ratio of A6OCB/C6M: 10, at real time

Movie S4: Circle/multicircle actuation by chloroform. Film length: 6 mm, width: 1 mm, thickness: 15 μm, molar ratio of A6OCB/C6M: 10, at real time

Movie S5: Actuation behavior of cross-shaped LCE-colloidal film by dichloromethane. Film length: 6 mm, width: 1 mm, thickness: 15 μm, molar ratio of A6OCB/C6M: 10, at real time

1.4 Characterization

The thermodynamic properties were characterized with differential scanning calorimetry (DSC6200) at heating and cooling rates of 5℃/min under nitrogen purge for the mixture and the pure LCE film. The thermal stability of the pure LCE film was tested by thermo-gravimetric analysis (TGA4000). The mesomorphic properties of the LC mixture and the pure LCE film were studied by polarizing optical microscopy (POM, Olympus, BX53) equipped with a hot stage (Linkam, THMS-600). The morphologies of LCE-colloidal film was observed by scanning electron microscopy (SEM, Japan Hitachi S-4800) operating at 10.0 kV. FTIR spectrum was recorded on an infrared spectrometer (Bruker, VERTEX 70, 36×, NA = 0.5). The water contact angle (CA) was measured on an OCA20 machine (DataPhysics, Germany) at ambient temperature with 2 μL water-drop measuring 3 times. The as-prepared LCE-colloidal film was cut into rectangles with length of 2, 4, 6, 8, 10 and 12 mm and width of 1 mm and then was immersed in a series of solvents (such as dichloromethane, chloroform, 1,2-dichloroethane, THF and acetone and water). The actuating process was observed with high-speed camera (GC-PX100BAC) taken at 60 fps.

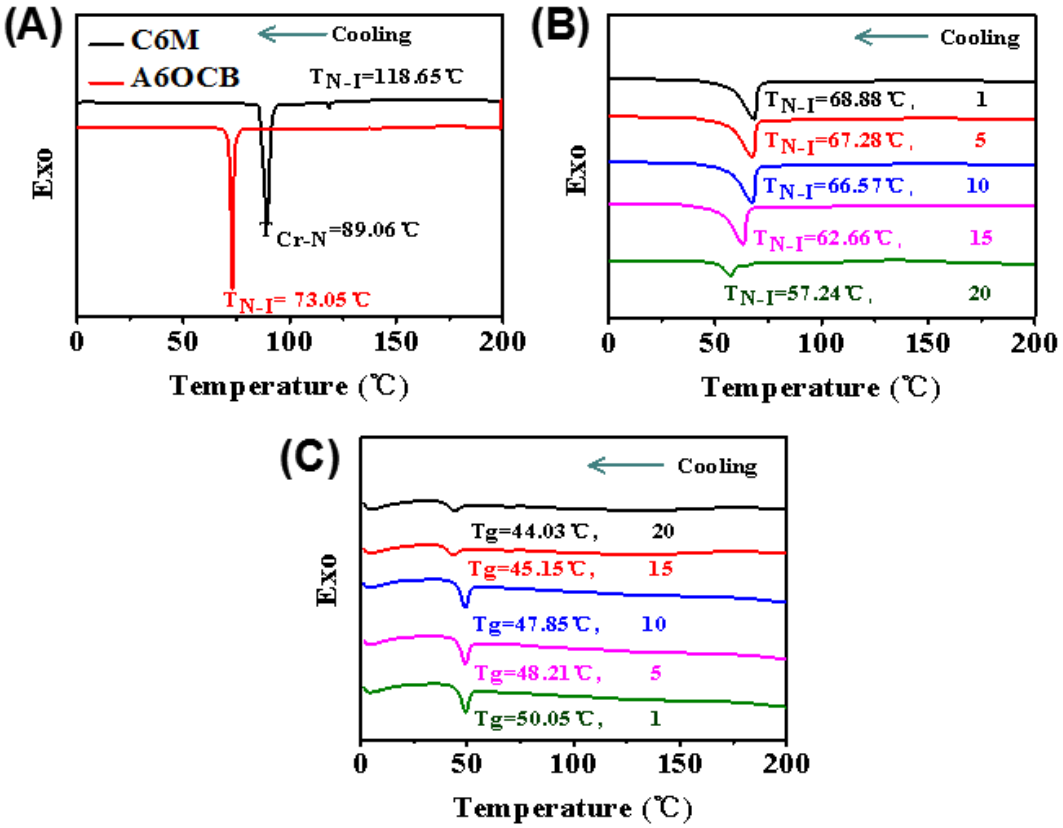

Fig. S1 DSC curves for (A) monomer A6OCB and cross-linker C6M (B) LC monomer mixture before photo-polymerization and (C) pure LCE. Inserted numbers are the molar ratio of A6OCB/ CM6 from 1 to 5, 10, 15 and 20.

To understand the thermodynamic properties and phase transition behavior of as-prepared sample, the thermal property of the monomer of A6OCB, cross-linker of C6M, LC mixture including A6OCB and C6M, and pure LCE were measured by DSC. The peak at 89.06℃ was resulted from the crystallization of C6M in **Fig. S1A**. The nematic-to-isotropic transition temperature (T_{NI}) was 118.65℃ and 73.05℃ for C6M and A6OCB, respectively in **Fig. S1A**. The endothermic peak shifted from 68.88℃ to 57.24℃ for LC mixture with molar ratio of A6OCB/C6M varying from 1 to 5, 10, 15 and 20 in **Fig. S1B**. Notably, the T_{NI} of pure LCEs was not observed before the thermal decomposition, this may be attributed that molecular alignment in LC phase was frozen in hot solid. The glass transition temperature (T_g) of pure LCE film (with molar ratio of A6OCB/C6M varying from 1 to 5, 10, 15 and 20) were also tested **and** changed from 50.05℃ to 48.21℃, 47.85℃, 45.15℃ and 44.03℃ in **Fig. S1C**, respectively. In addition, as a permanent cross-linker, C6M could be incorporated into the LC network to increase mechanical coherence of the actuator, which could provide chemical resistance, mechanical stability and shape reversibility. Otherwise, the cross-linker could inhibit the formation of smectic phase with interference in photo-polymerization process.

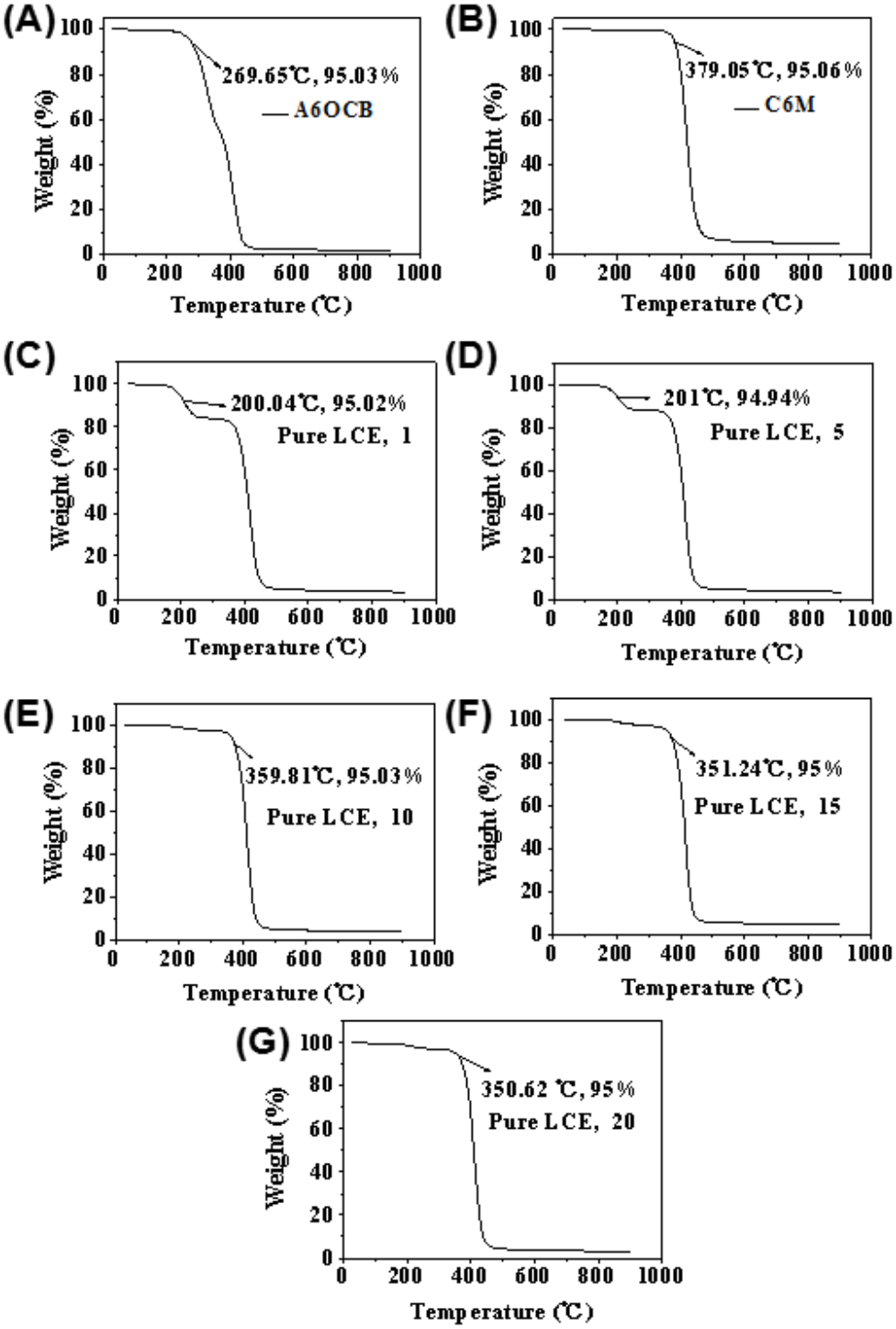

Fig. S2 TGA curves of (A) LC monomer A6OCB, (B) LC cross-linker C6M and (C-G) pure LCE film with molar ratio of A6OCB/C6M from 1 to 5, 10, 15 and 20.

TGA analyses showed that mass loss of pure LCE film was less than 5 wt% for sample with molar ratio of A6OCB/C6M varying from 1 to 5, 10, 15 and 20. Above-mentioned LCE films had good thermal stability, with the thermal decomposition temperature of 200.04℃, 201℃, 359.81℃, 351.24℃ and 350.62℃, respectively.

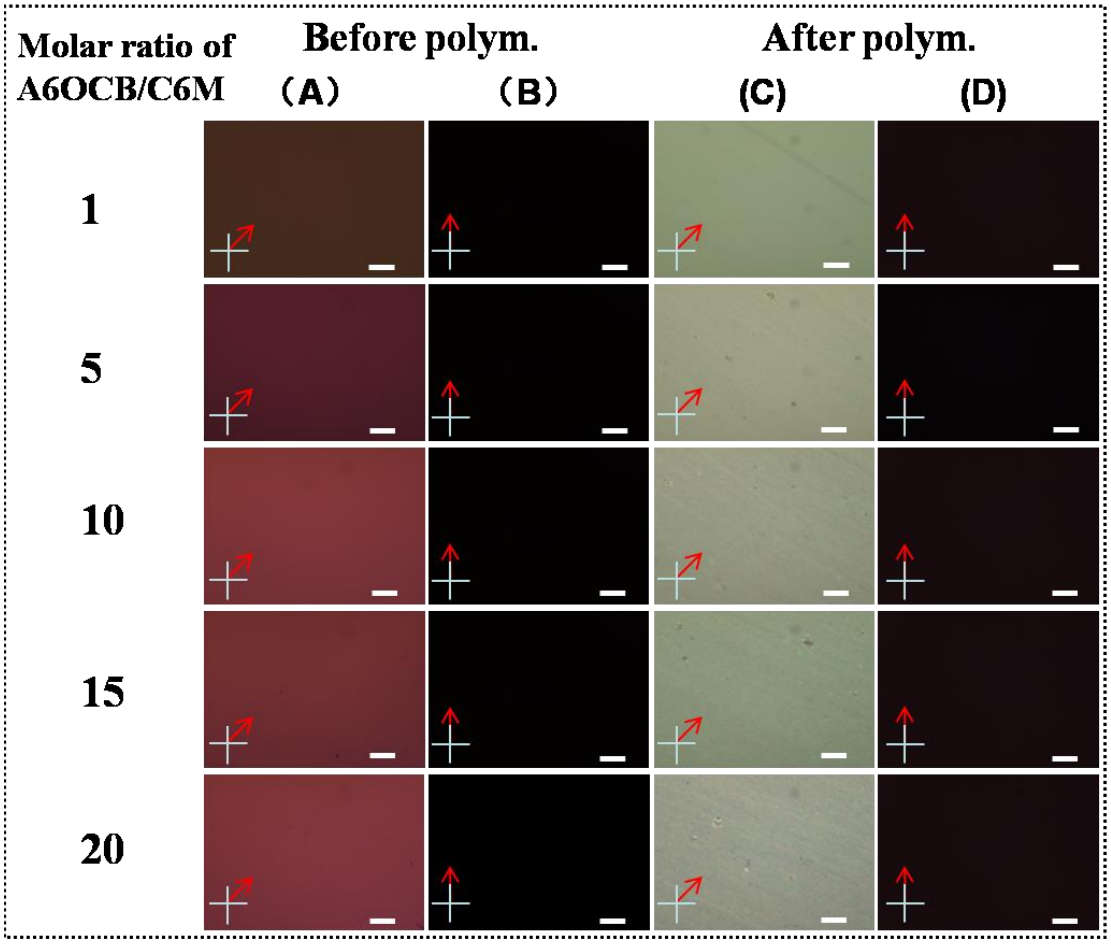

Fig. S3 POM images of sample with molar ratio of A6OCB/C6M varying from 1 to 5, 10, 15 and 20 in the LC cell before (A and B) and after photopolymerization (C and D) with their rubbing directions at (A and C) 45° and (B and D) 0° from the polarizer. The scale bar is 100 μm.

The alternation images of bright and dark for sample with molar ratio of A6OCB/C6M (at 1, 5, 10, 15 and 20) were observed through rotating objective table before photopolymerization, which indicated that the planar orientation LC cell could induce the orientation of A6OCB/C6M mixture along the rubbing direction. After photopolymerization, the samples also had bright and black fields. So the texture of nematic LC was completely maintained by cross-linked LC polymers.

2.Anisotropic swelling of LCE-colloidal film

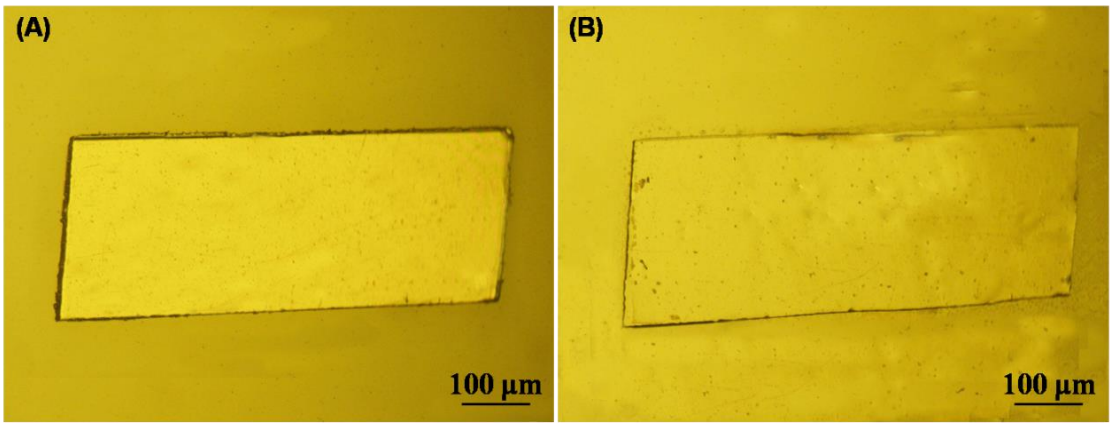

Fig. S4 Optic microscopy images of LCE-colloidal film before (A) and after (B) being immersed in dichloromethane. The dimension of the sample can be visually changed after being immersed into dichloromethane.

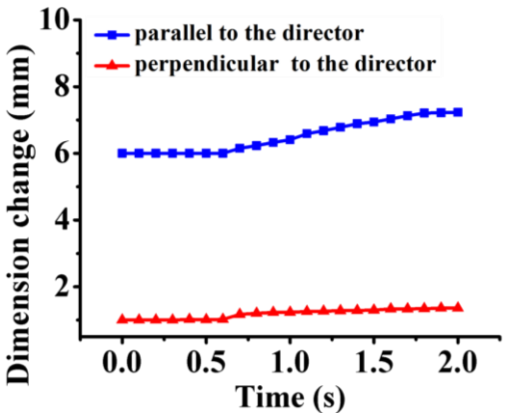

Fig. S5 The change of the dimension of the geometric axis of the homogeneously aligned LCE-colloidal film with dimension of 6 mm × 1 mm × 15 μm. The size change of LCE-colloidal film was recorded after the sample being immersed in dichloromethane. The long geometric axis of the LCE-colloidal film is parallel to the LC molecule director. The blue and red curves represent the size changes of the LCE-colloidal film parallel and perpendicular to the director, respectively.

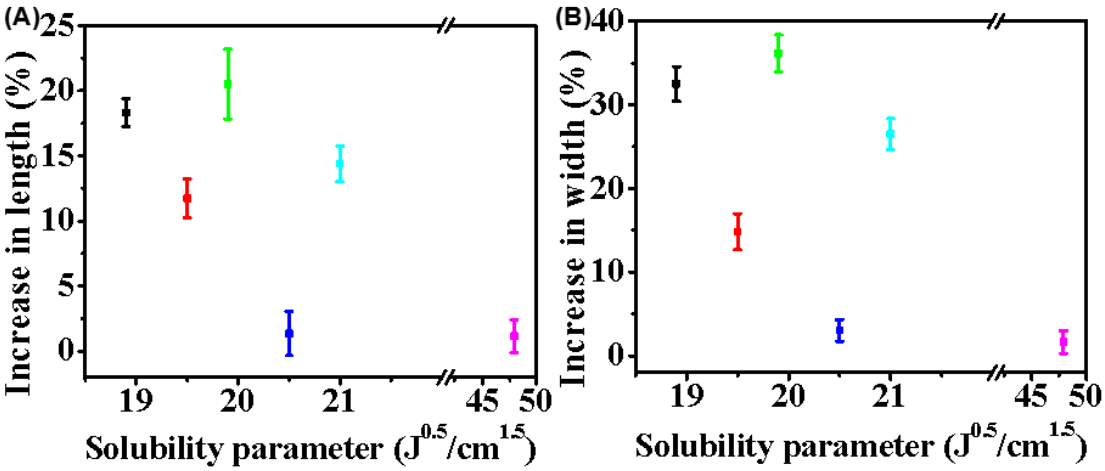

Fig. S6 The increase of percentage in the long geometric axis (A) and short geometric axis (B) of LCE-colloidal film in various solvents as a function of the solubility parameter of solvents. The color lines in the graph respectively represent chloroform (black line), THF (green line), dichloromethane (indigo line), acetone (red line), 1, 2-dichloroethane (blue line) and water (pink line).

Fig. S6 shows the swelling of a plane oriented LCE-colloidal film. Because of the difference of elasticity modulus, the swelling degree of the film perpendicular to director direction was greater than that of the film parallel to the director direction. Meanwhile, the solvent type would also affect the swelling degree of the film. It could be seen from **Table 1** that dichloromethane could make the LCE-colloidal film swell to the maximum extent.

Table 1. Size change of long and short geometric axis of LCE-colloidal film. The long geometric axis of the LCE-colloidal film is parallel to the LC molecules director.

Organic solvent	Increase in short geometric axis /%	Increase in long geometric axis /%	α	γ
Dichloromethane	36.12±2.23	20.51±2.67	2.23	1.13
Chloroform	32.49±2.06	18.31±1.08	2.08	1.11
1,2-dichloroethane	26.51±1.86	14.38±1.38	1.83	1.11
THF	14.83±2.13	11.73±1.49	1.47	1.02
Acetone	3.04±1.28	1.35±1.70	1.08	1.01
Water	1.65±1.36	1.15±1.27	1.04	1.00

The total volume change of the LCE-colloidal film was expressed as α. $\alpha = V/V_0$, V is the swelling volume, and V_0 was the volume of the original film. This calculation assumed that the change the thickness of the sample was similar to that of the short geometric axis of the sample. The actuation anisotropic formula was as follows:

$$\gamma = \frac{L_{f\perp}}{L_{o\perp}} \Big/ \frac{L_{f//}}{L_{o//}} \tag{1}$$

L_0 was the length of the long geometric axis of the original LCE-colloidal film, and L_f was the length of the final swelling of the film. "//" and "⊥" indicate parallel or perpendicular to the director, respectively.

3. Actuation behavior of LCE-colloidal film

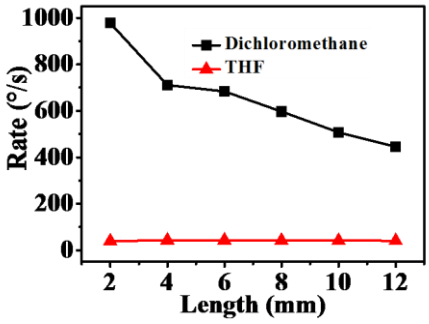

Fig. S7 The actuation rate of LCE-colloidal film (1 mm ×15 μm, the molar ratio of A6OCB/C6M of 10) under LCE-colloidal film with length of 2, 4, 6, 8, 10 and 12 mm in dichloromethane and THF, respectively.

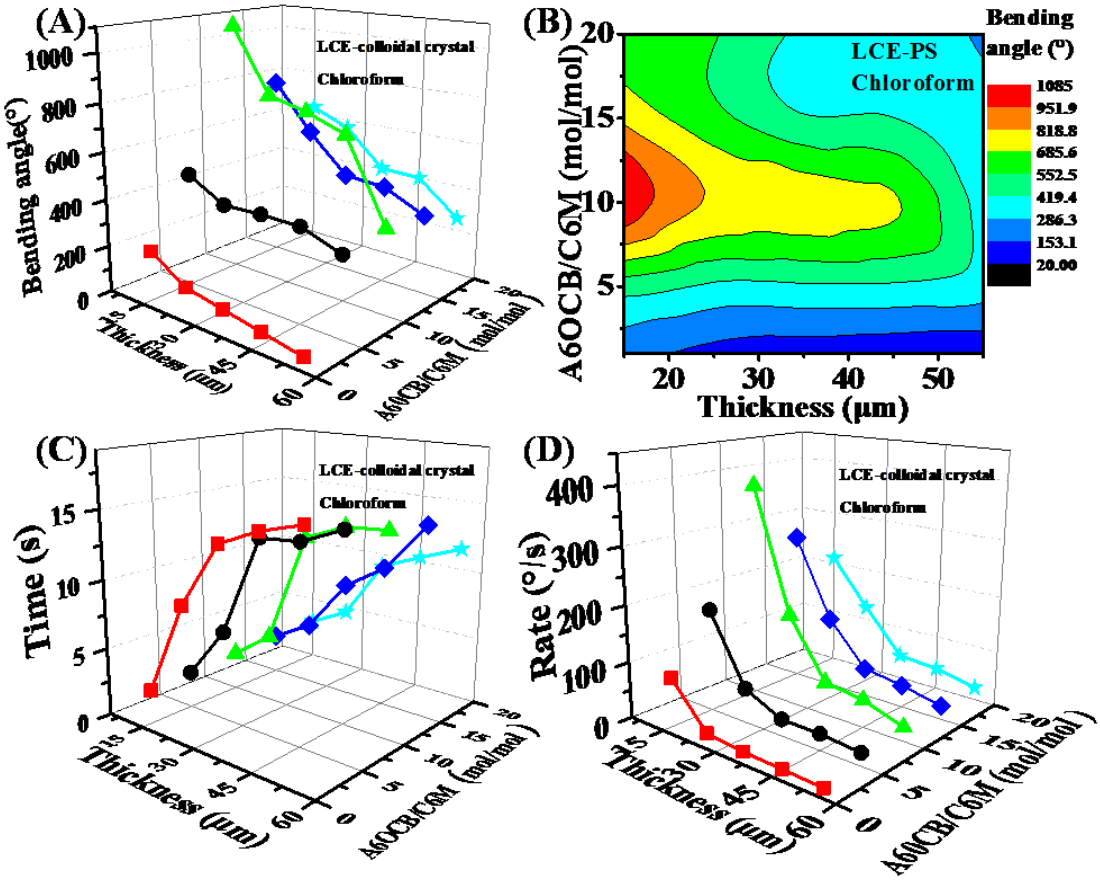

Fig. S8 (A and B) The BA_{max}, (C) the actuation time achieving the BA_{max} and (D) the actuation rate of LCE-colloidal film with various molar ratio of A6OCB/C6M, with thickness of 15, 25, 35, 45 and 55 μm in chloroform.

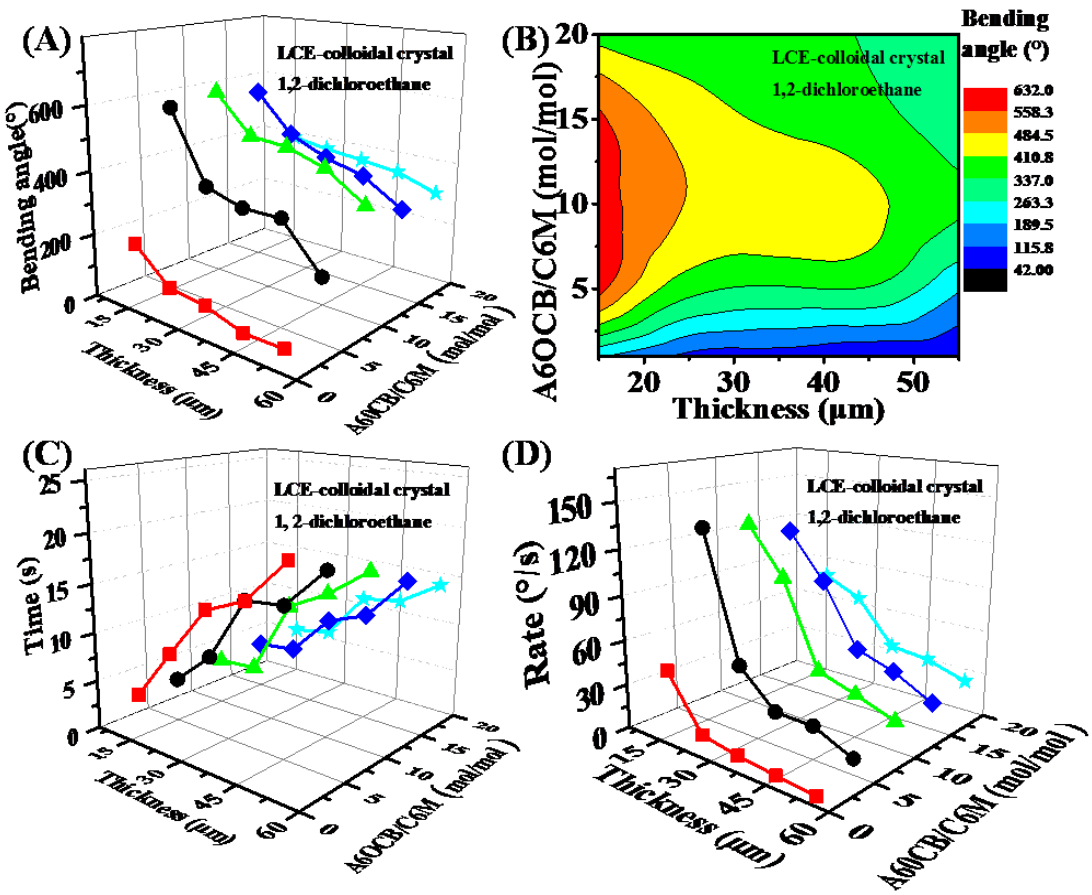

Fig. S9 (A and B) The BA_{max}, (C) the actuation time achieving the BA_{max}, and (D) the actuation rate of LCE-colloidal film with various molar ratio of A6OCB/C6M, with thickness of 15, 25, 35, 45 and 55 μm in 1,2-dichloroethane.

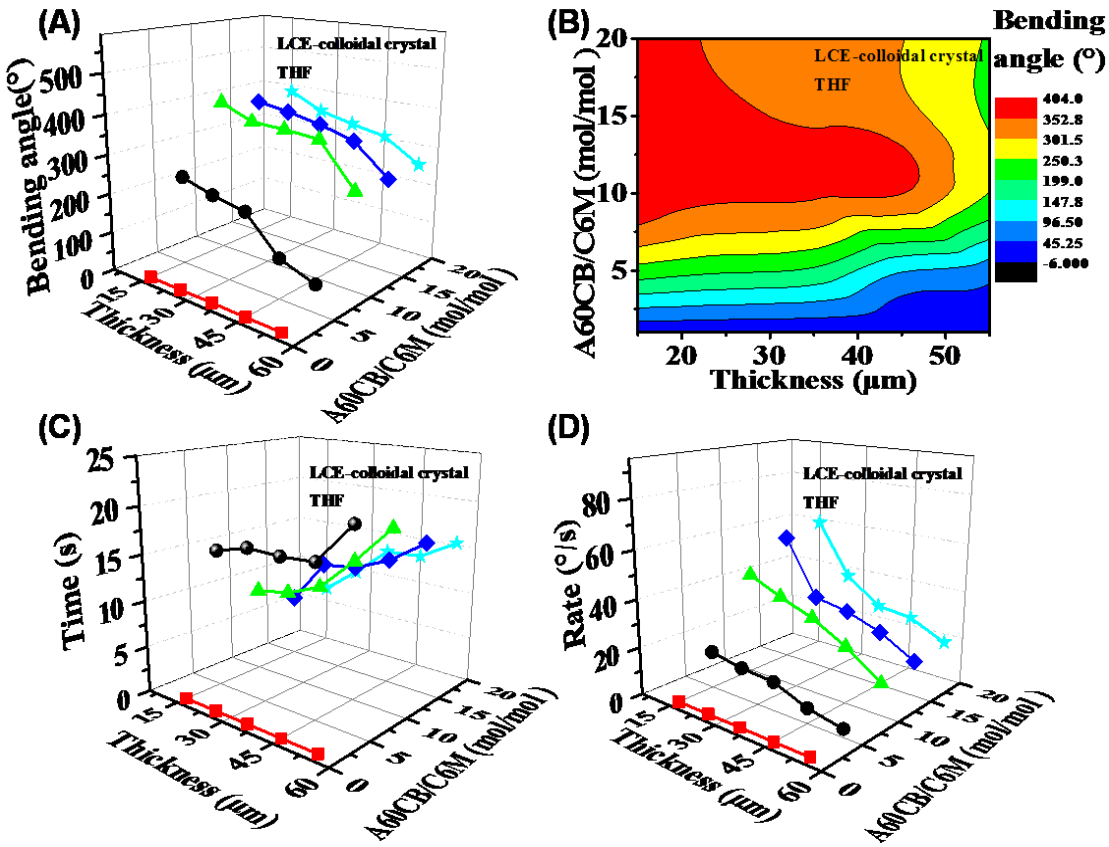

Fig. S10 (A and B) The BA_{max}, (C) the actuation time achieving the BA_{max}, and (D) the actuation rate of LCE-colloidal film with various molar ratio of A6OCB/C6M, with thickness of 15, 25, 35, 45 and 55 μm in THF.

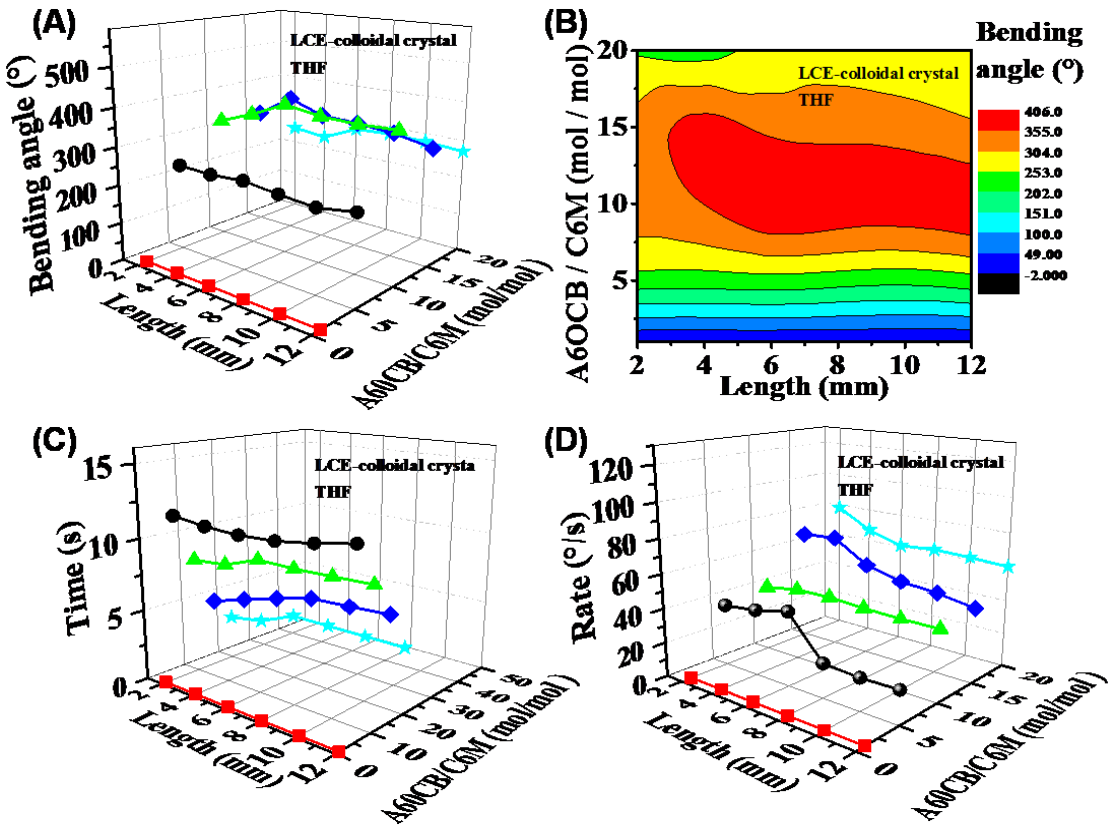

Fig. S11 (A and B) The BA_{max}, (C) the actuation time achieving the BA_{max}, and (D) the actuation rate of LCE-colloidal film with various molar ratio of A6OCB/C6M, with length of 2, 4, 6, 8, 10 and 12 mm in THF.

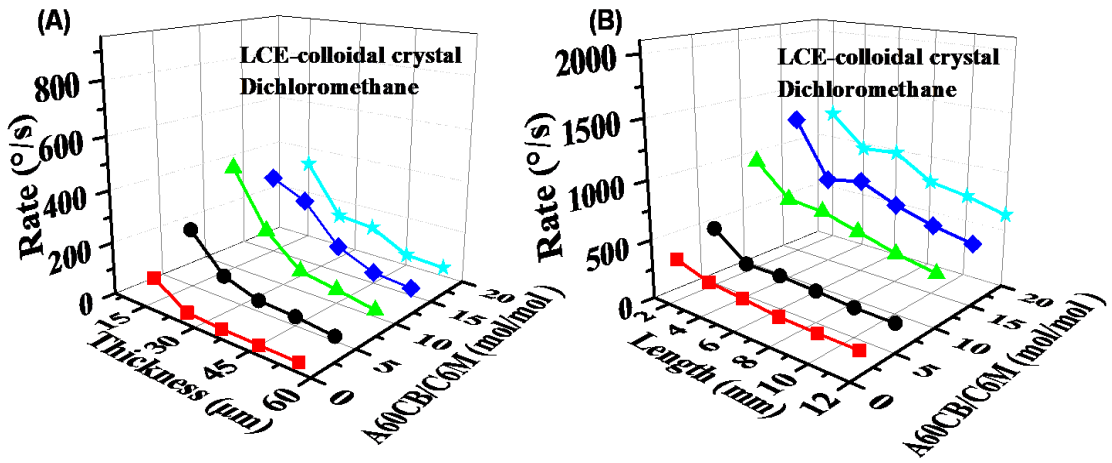

Fig. S12 The actuation rate of LCE-colloidal film with various molar ratio of A6OCB/C6M, (A) film with thickness of 15, 25, 35, 45 and 55 μm and (B) film with length of 2, 4, 6, 8, 10 and 12 mm in dichloromethane.

4.Stress-strain curves of LCE-colloidal

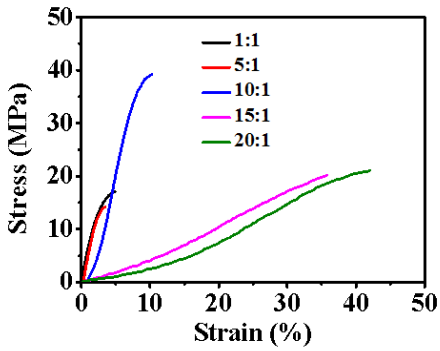

Fig. S13 Stress-strain curves of LCE-colloidal with the molar ratio of A6OCB/ CM6 from 1 to 5, 10, 15 and 20.

5.Recyclability of LCE-colloidal film

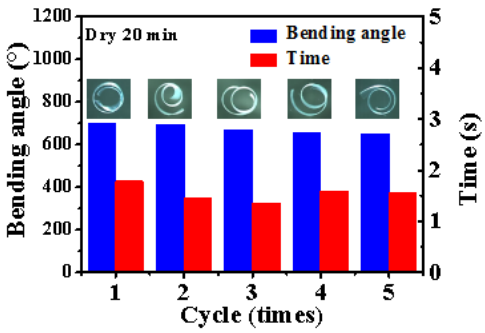

Fig. S14 The actuation time and bending angle taken for LCE-colloidal film approaching the BA_{max} in dichloromethane for the first five cycles. The insert is the images of the BA_{max} in corresponding actuation process.

As the number of cycles increases, the BA_{max} decreased gradually due to the collapse of the macroporous structure after multiple immersion of solvent.

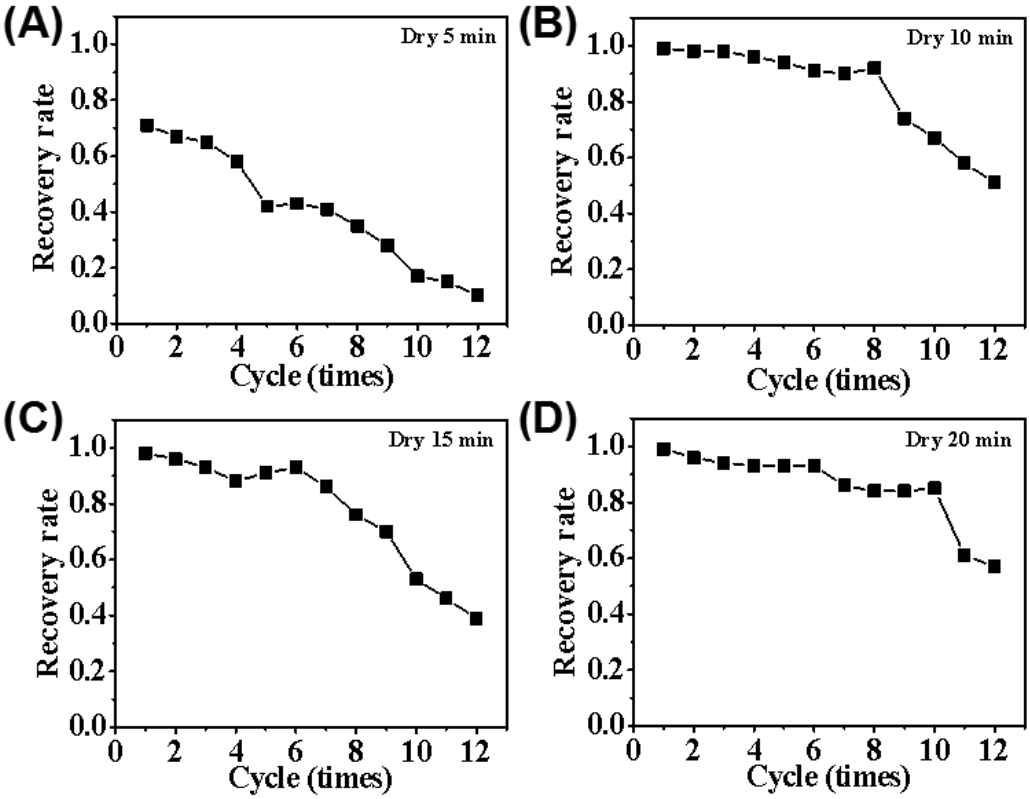

Fig. S15 The recovery rate of bending angle of the LCE-colloidal film after drying for (A) 5 min, (B) 10 min, (C) 15 min and (D) 20 min, respectively.

When the sample with being immersed in dichloromethane for the first time is dried in oven for 5 min, the recovery rate of bending angle of the film only reaches to 0.71 because the solvent was not volatilized from the film completely. After 12 cycles, the recovery rate decreases to 0.1. In contrast, after being dried for 10 min, 15 min and 20 min, the recovery rate was 0.99, 0.98 and 0.99 respectively. It can be seen that the time taken to dry the sample has an important effect on the recovery rate of bending angle.

6.Control of bending angle by composition of different solvents

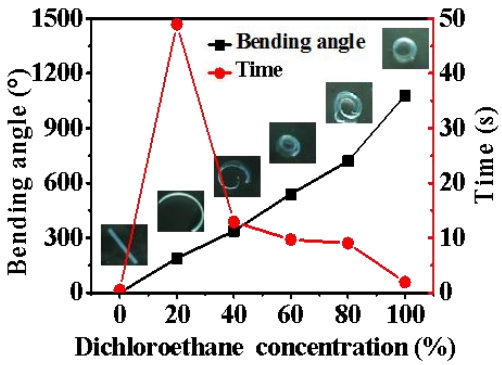

Fig. S16 The BA_{max} of the LCE-colloidal film at different dichloromethane concentration in dichloromethane-ethanol mixture. The inserted images are the photos of LCE-colloidal film with the BAmax after being immersed in the corresponding solvent.

The BA_{max} of LCE-colloidal film rose from 0° to 188.35°, 337.82°, 540°, 720° and 1080° with the increase of dichloromethane concentration in dichloromethane-ethanol mixture system, which indicates the BA_{max} of LCE-colloidal film as a function of solvent concentration. With the increase of dichloromethane volume fraction, the *BA* of the film raised, which indicated that the LCE-colloidal film can be used as a rapid response macroscopic quantitative indicator to measure the ethanol content in the mixed system.

7.SEM images of the LCE-colloidal film after being immersed in dichloromethane

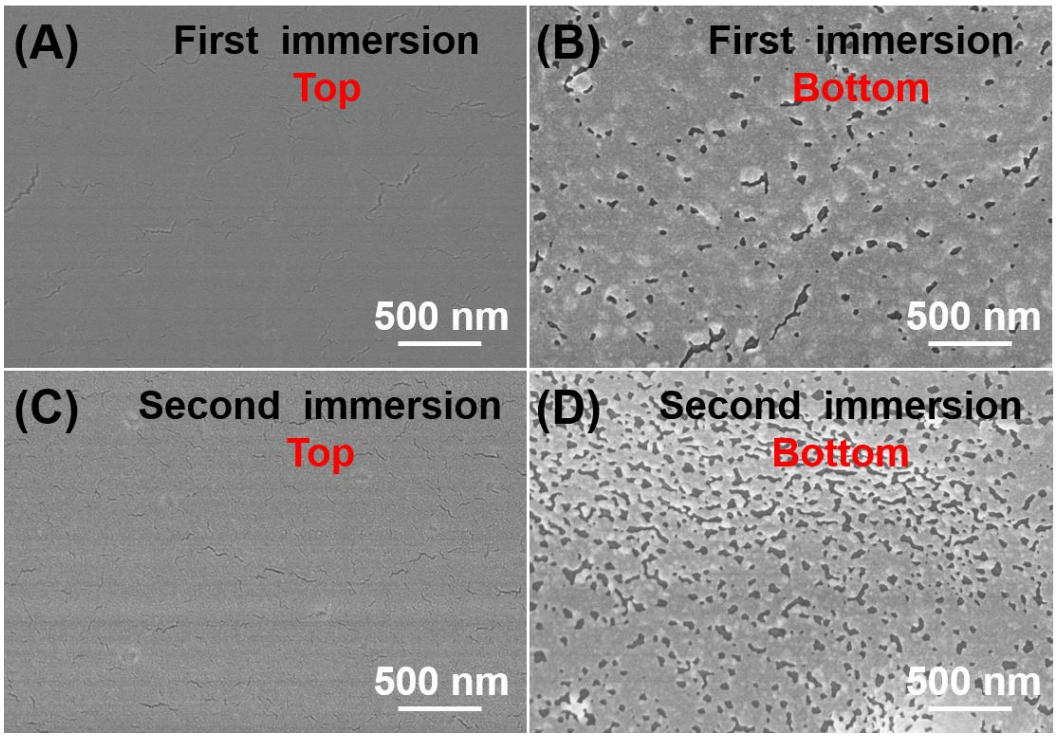

Fig. S17 SEM images of the top and bottom surfaces of the LCE-colloidal film after being immersed in dichloromethane once and twice.

After the sample was first immersed into solvent, the top surface of the LCE-coloidal is a smooth bulk LCE layer, while the bottom surface is a rough porous structure due to the dissolution of polymer microspheres. After the second immersion, the area of the pore structure on the bottom surface increases, indicating the further dissolution of the polymer particles.

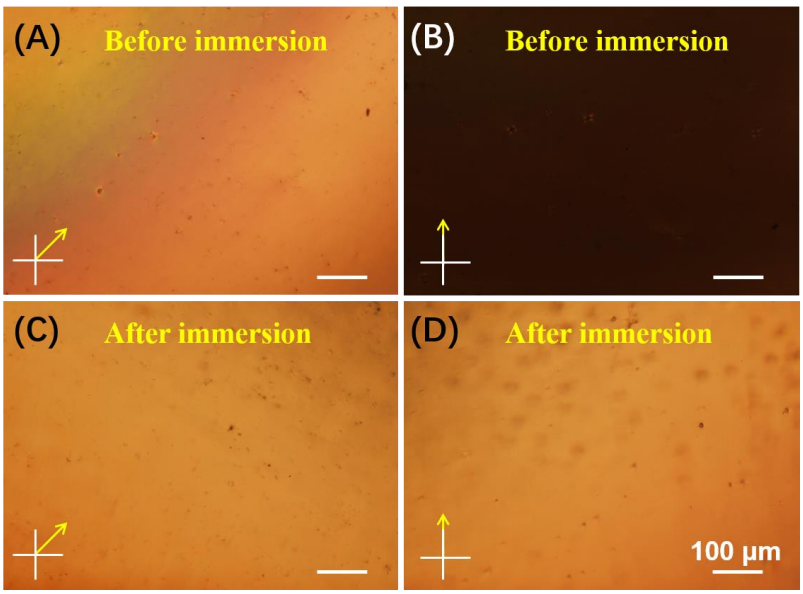

Fig. S18 POM images of sample before (A and B) and after (C and D) being immersed in dichloromethane with their rubbing directions at (A and C) 45° and (B and D) 0° from the polarizer.

The light could transmit through the polarizers and the brightness obviously changes when LCE-colloidal film is rotated by 45° in (A) and (B) before being immersed. However, we do not observe a significant change in brightness after the sample being immersed by rotating 45°. It shows that the sample has a good plane alignment before being immersed, but the alignment order decreases after being immersed. During solvent immersion, the sample undergoes an order-disorder phase transition.

8.Actuation mechanism of LCE-colloidal and pure LCE film

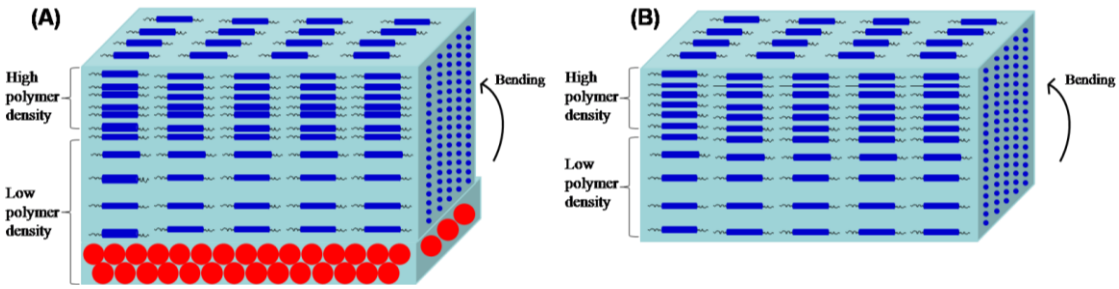

Fig. S19 Schematic diagram of actuation behavior of LCE-colloidal film (A) and pure LCE film (B) based on UV intensity gradient.

9.Thermal polymerization

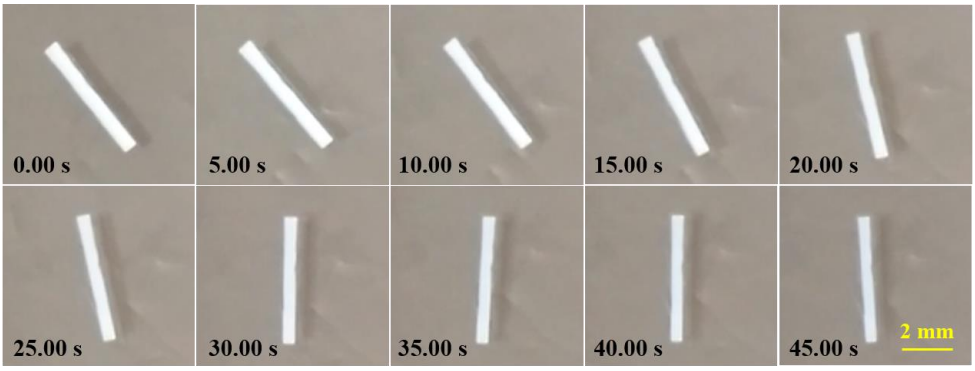

Fig. S20 Actuation behavior of plane oriented pure LCE prepared by thermal polymerization in dichloromethane.

Monomer of C6M, cross-linker of A6OCB and thermal initiator of AIBN are dissolved in chloroform under the protection of N_2. The mixture is injected in LC cell obtained by two glass substrates coated of a rubbing treated PI alignment layer. Thermal polymerization is carried out at 70℃ for 4 h. When the pure LCE film obtained by the thermal polymerization is placed in the dichloromethane, the film doesn't bend because the uniaxially oriented pure LCE obtained by thermal polymerization is equivalent in response to dichloromethane in all regions. It is proved that the UV intensity gradient in the original system leads to the bending of pure LCE films.

10. Demonstration of bending direction of the LCE-colloidal film for β=0°

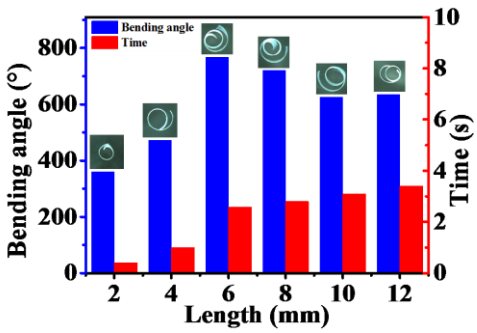

Fig. S21 Experimental results for the BA_{max} of LCE-colloidal film (1 mm × 15 μm) as a function of LCE-colloidal film with length of 2, 4, 6, 8, 10 and 12 mm in dichloromethane.

11.Effect of colloidal particles on the orientation of liquid crystal molecules

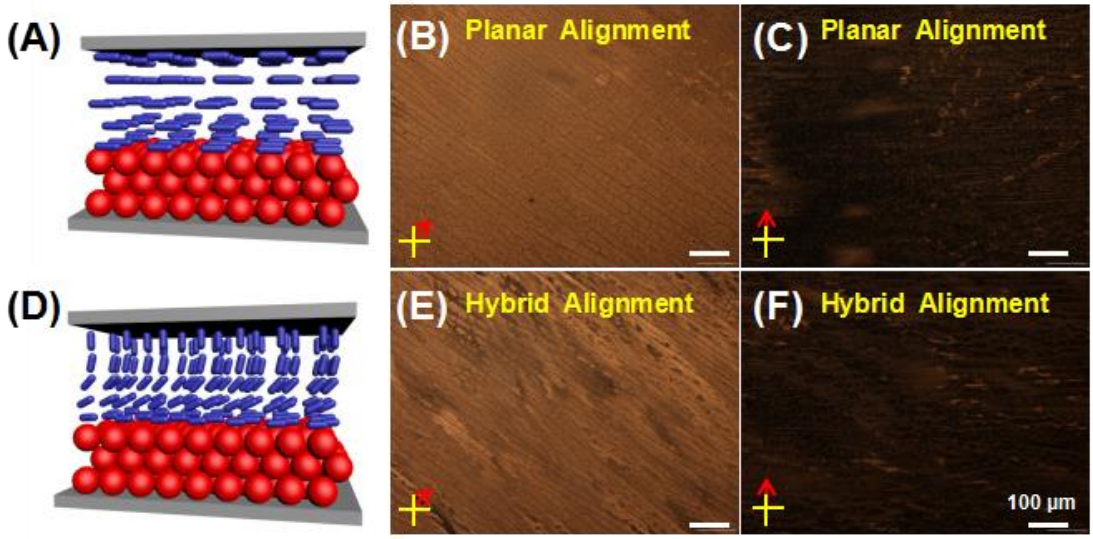

Fig. S22 (A and E) The schematic diagram of two kinds of LC cell. (B, C, E and F) The POM images of LCE-colloidal with (B and C) planar and (E and F) perpendicular alignment by rotating samples from 45° to 90°, respectively.

Planar and perpendicular oriented LC cells are prepared by combination of parallel /perpendicular oriented glass and colloidal particle template to investigate the effect of colloidal surface on LC molecules orientation. In this experiment, 5CB, presenting LC state at room temperature, is used as the tested LC. Two kinds of LC cells are observed under a polarizing optical microscope, it was found that alternated light and dark field appears by rotating the sample at 45°. It can be proved that colloidal surface has a plane-induced effect on the LC molecules.

12.Actuation behavior of pure LCE film

12.1 Three shear modes of LCE film

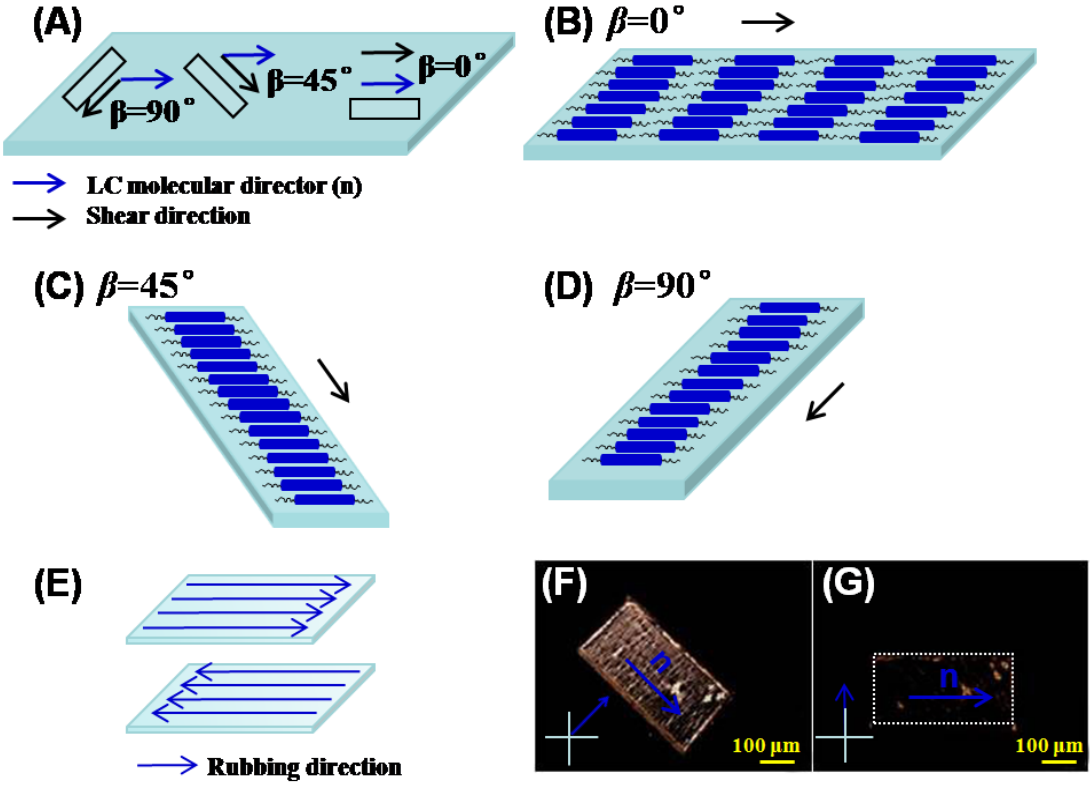

Fig. S23 (A-E) Schematic diagram of pure LCE film (A) shear direction and molecular orientation of LCE film. Black and blue arrows represent the shear direction and molecular director, respectively. (B-D) Pure LCE based on the angle (β= 0°, 45° and 90°) between LC molecular director and shear direction. (E) LC molecules on the upper and lower surfaces in a plane oriented LC cell. (F and G) POM images of pure LCE with LC molecular plane orientation and their rubbing directions at (F) 45° and (G) 0° from the polarizer.

LCE films always bent along the short axis of LC molecules because of the difference of elastic modular between long and short axis of LC molecules. Moreover, the bending direction of film was also related to the UV intensity gradient. Three kinds of shear directions were designed here to explore different actuation behavior.

12.2 Actuation images of pure LCE film

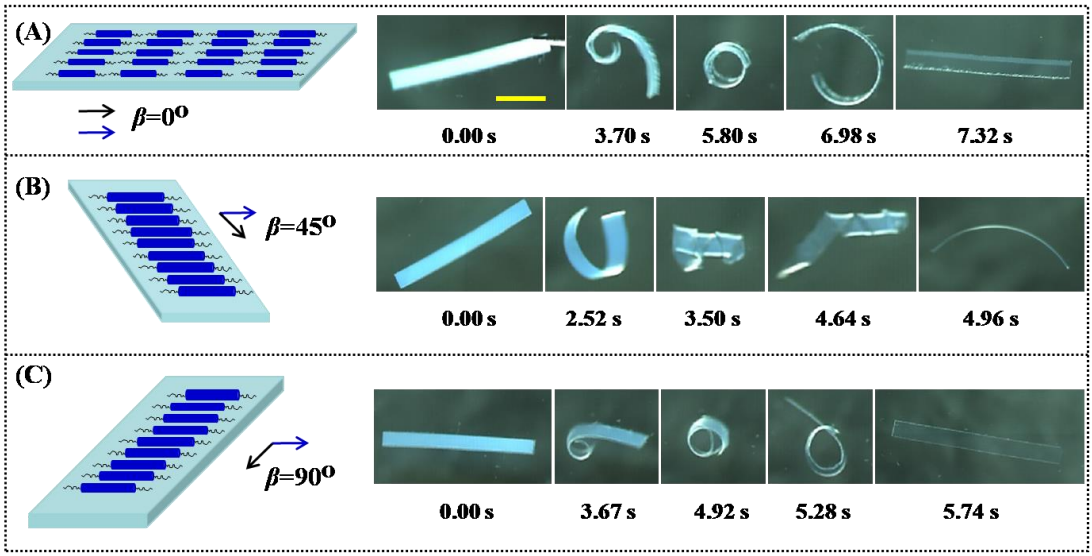

Fig. S24 Left: (A-C) Schematic diagram of the LC molecules alignment and shear direction. Right: (A-C) Actuation images of pure LCE film (1 mm × 6 mm × 15 μm) in response to dichloromethane. The scale bar is 2 mm.

The shear direction of the film was closely related to actuation behavior, which was due to the difference of the elasticity modulus perpendicular and parallel to the director.